



## Malaysian Journal on Composites Science and Manufacturing

Journal homepage:  
<https://karyailham.com.my/index.php/mjcsm/index>  
ISSN: 2716-6945



# Evaluation of Structural and Electrochemical Performance of $Ti_3C_2$ MXene/ $MoS_2$ Electrode in PVA-based Solid Electrolyte

Muhammad Akmal Kosnan<sup>1</sup>, Mohd Asyadi Azam<sup>1,\*</sup>, Nur Ezyanie Safie<sup>2</sup>, Rose Farahiyan Munawar<sup>1</sup>, Intan Sharhida Othman<sup>1</sup>, Jeefferie Abd Razak<sup>1</sup>, Akito Takasaki<sup>3</sup>, Muhammad Faizadmesa Allim<sup>1</sup>

- <sup>1</sup> Fakulti Teknologi dan Kejuruteraan Industri dan Pembuatan, Universiti Teknikal Malaysia Melaka, Hang Tuah Jaya, 76100 Durian Tunggal, Melaka, Malaysia  
<sup>2</sup> Fakulti Teknologi dan Kejuruteraan Elektrik, Universiti Teknikal Malaysia Melaka, Hang Tuah Jaya, 76100 Durian Tunggal, Melaka, Malaysia  
<sup>3</sup> Department of Engineering Science and Mechanics, College of Engineering, Shibaura Institute of Technology, 3-7-5 Toyosu, Koto-Ku, Tokyo 135-8548, Japan

### ARTICLE INFO

#### Article history:

Received 28 May 2025  
Received in revised form 11 July 2025  
Accepted 15 July 2025  
Available online 30 July 2025

#### Keywords:

MXene,  $MoS_2$ , Characterization, Symmetric Supercapacitor, Polymer Electrolyte

### ABSTRACT

Solid electrolytes have gained significant interest for the use in supercapacitor application. The unique blend of its characteristics ensures excellent durability and long-lasting performance. However, the complex synthesis process required for these electrolytes has limited the prospect. This study aims to develop a high-performance solid-state supercapacitor by synergistically combining a PVA-based solid electrolyte with a MXene/ $MoS_2$  composite electrode. The key challenges are to achieving a good compatibility between the flexible PVA electrolyte and layered MXene/ $MoS_2$  electrode to prevent delamination and understanding ion transport through PVA's hydrophilic network and MXene/ $MoS_2$ 's hierarchical structure, while ensuring long-term capacitance retention. A low-energy hydrothermal synthesis approach is used to enable scalable and greener fabrication. Confirmation of the characterization for the synthesized MXene and  $MoS_2$  composite was achieved through X-ray Diffraction and Raman analysis. While Field Emission Scanning Electron Microscope were employed to examine the morphology. The highest specific capacitance recorded was 50.62 Fg<sup>-1</sup>, attributed to the higher ionic conductivity and better mechanical properties of PVA based solid electrolyte in utilizing 2D material. Moreover, the device demonstrated almost 95.75% retention of its original capacitance upon a 10,000-cycle cyclic stability test at high current.

## 1. Introduction

Supercapacitors (SC) serve as crucial energy storage devices, akin to traditional capacitors in many respects. However, their operational mechanism distinguishes them from regular capacitors. SCs

\* Corresponding author.

E-mail address: [asyadi@utem.edu.my](mailto:asyadi@utem.edu.my)(Mohd Asyadi Azam)

<https://doi.org/10.37934/mjcsm.17.1.2137>



In this study, we propose a solid-state supercapacitor system that synergistically combines a PVA-based solid electrolyte with a composite MXene/MoS<sub>2</sub> electrode. Analytical techniques such as FESEM, Raman, and XRD will be employed to investigate this correlation.

It is important to note that the focus of this study is not an exhaustive optimization of the synthesis procedure. Rather, it aims to explore the synergistic effect of the composite material, introducing specific enhancements strategically crafted to address identified limitations and build upon existing knowledge. For the case where MXene is hybridized with MoS<sub>2</sub>, it is noted by [39] that this pair able to utilize the reciprocal dispersion in the interlayer of nanosheets to solve the stacking problem, while minimizing issues of restacking for both materials in long cycles of charge/discharge testing or application. This is due to this hybridization strategy that offered synergistic effect [39] and tunability in various properties from the enhanced multifunctional hierarchical structure [40-45] coming from MXene/MoS<sub>2</sub> combination. PVA-based solid electrolytes play a crucial role in enhancing the performance of supercapacitors. These polymer electrolytes offer several advantages that contribute to the efficiency and stability of supercapacitor devices. PVA-based solid electrolytes exhibit high ionic conductivity, which is essential for efficient charge transfer within supercapacitors. This high conductivity enables rapid movement of ions, enhancing the energy storage and delivery capabilities of the supercapacitor. PVA solid electrolytes provide flexibility, allowing for their use in flexible solid-state supercapacitors [18]. This flexibility expands the range of applications where supercapacitors can be utilized, making them suitable for various electronic devices and systems. The prevalent ionic conductivities of polymer electrolytes based on PVA are displayed in Table 1. Inspired by the considerations above, this paper outlines the novelty of current study that utilize three-way concerted exploration in 1) facile synthesis of MXene/MoS<sub>2</sub> hybrid, 2) sustainable approach to produce solid electrolyte, and 3) ion intercalation evaluation via solid electrolyte with MXene-MoS<sub>2</sub> electrode in supercapacitor applications.

**Table 1**  
The ionic conductivities of electrolytes based on PVA

Electrolyte	Ionic conductivity (m Scm <sup>-1</sup> )	Ref
PVA/H <sub>3</sub> PO <sub>4</sub> /H <sub>2</sub> O	0.056	[19]
PVA/Potassium Borate/ KCL/H <sub>2</sub> O	1.02	[20]
PVA/H <sub>3</sub> PO <sub>4</sub> /cellulose/H <sub>2</sub> O	0.104	[21]
PVA/PVP/KOH/H <sub>2</sub> O	1.5 x 10 <sup>-1</sup>	[22]

## 2. Methodology

### 2.1 Synthesis Method MXene, MoS<sub>2</sub> and PVA based solid electrolyte

The experimental methodology is schematically illustrated in Figure 2.

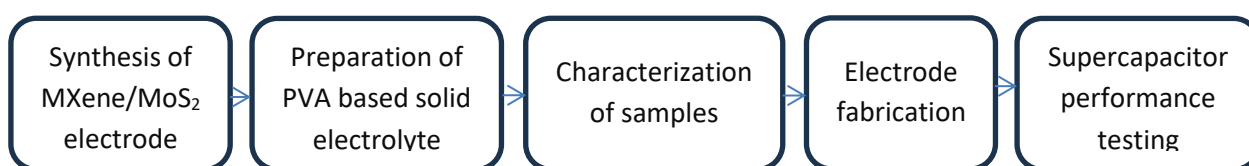


**Fig. 2.** Flowchart of the experiment

Titanium aluminum carbide ( $Ti_3AlC_2$ ) MAX phase powders were slowly submerged in a 40 wt% hydrofluoric acid (HF) solution under constant stirring for 24 hours at room temperature. This process facilitates the selective etching of aluminum layers from the MAX phase structure. The resulting suspension was then centrifuged at 4000 rpm for 5 minutes and thoroughly washed with deionized (DI) water multiple times to remove residual fluoride ions and terminate the etching reaction. The washing steps were repeated until the supernatant reached a pH value exceeding 6.0, indicating the removal of excess HF. The final MXene ( $Ti_3C_2$ ) product was dried in a vacuum oven at 60°C for 12 hours. Then, a homogeneous solution of  $MoS_2$  was prepared through a hydrothermal method. While there are various routes of single MXene synthesis or hybridization with  $MoS_2$  such as chemical vapor deposition (CVD) [42, 43], atomic layer deposition (ALD), molten salt etching and hydrothermal method [43]. It is noted that CVD and ALD involve high-end instruments [42] and molten salt etching dealt with several synthesis steps with high risk of health hazards [43]. Hydrothermal synthesis method on the other hand has low-cost [45], facile [43, 44], secure, safe and environmentally friendly attributes [42]; making hydrothermal method is preferably recommended as synthesis protocol. Thiourea and ammonium molybdate tetrahydrate ( $(NH_4)_6Mo_7O_{24}\cdot 4H_2O$ ) were dissolved in DI water under vigorous stirring. The resulting mixture was transferred to a Teflon-lined stainless-steel autoclave and heated to 210°C for a reaction time of 40 minutes, followed by a holding period of 18 hours. The autoclave was then allowed to cool down naturally to room temperature. This process promotes the formation of  $MoS_2$  nanosheets.

## 2.2 Preparation of PVA Based Solid Electrolyte

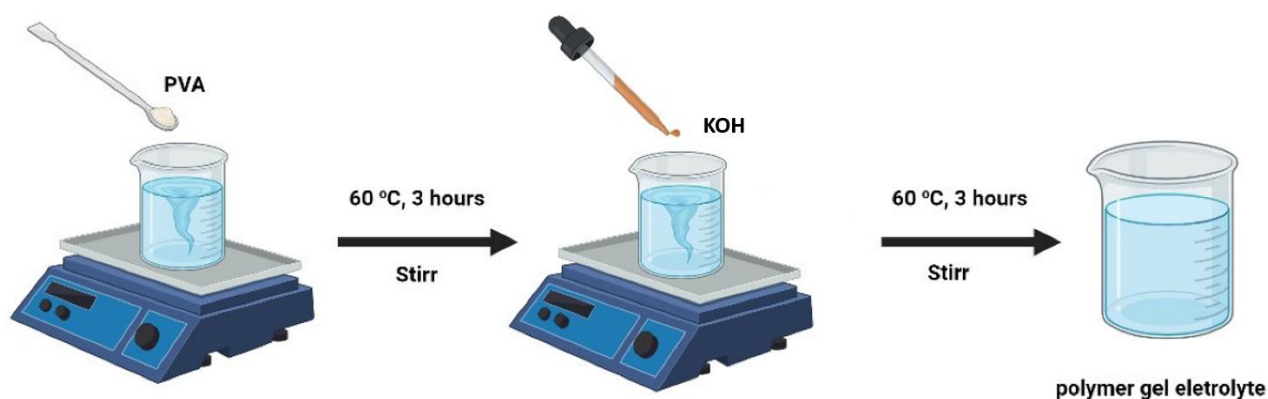
The PVA/KOH-based Solid electrolyte was synthesized via a solution-casting method (Figure 2). A mixture of 20 g polyvinyl alcohol (PVA) was dissolved in 300 mL of DI water under constant stirring at 60°C for 3 hours, as illustrated in Figure 3. The suspension was stirred for an additional three hours with 10 g of KOH added. The elevated temperature facilitates the dissolution of both components and ensures a homogeneous mixture. The stirring process continued until a clear and transparent solution was obtained, indicating complete dissolution. This method yields a PVA/KOH-based Solid electrolyte suitable for various electrochemical applications, including supercapacitors and batteries. After that, the electrolyte is poured into a petri dish to dry and form a thinner layer.

## 2.3 Preparation of $MoS_2/Ti_3C_2$ MXene Hybrid Electrode

Pre-synthesized  $MoS_2$  powder was thoroughly mixed with 0.13 g of  $Ti_3C_2$  MXene in an N-methylpyrrolidone (NMP) solution using constant stirring. This process promotes the uniform dispersion of  $MoS_2$  particles onto the MXene surface. The resulting homogeneous mixture was then transferred into a Teflon-lined stainless-steel autoclave with a capacity of 28 mL for a subsequent hydrothermal treatment (Figure 4). The following hydrothermal treatment steps were identical to those employed for the sole synthesis of  $MoS_2$  (refer to Section 2.1).

Several pre-prepared chemicals were utilized for the fabrication of the electrode slurry with electrode formulation and experiment parameters that were adopted with minor changes at stirring time, referred from past literature study [41]: polyvinylidene fluoride (PVDF) binder, acetylene black conductive agent, NMP solvent, and PVA-based based Solid electrolyte. The slurry was formulated using a fixed weight ratio: 80 wt% active material, 10 wt% PVDF binder, and 10 wt% acetylene black conductive additives. When the active material employed was the  $MoS_2$ /MXene composite, the individual components ( $MoS_2$  and MXene) were mixed in equal proportions (50 wt% each) based

on prior research that established this ratio as optimal for achieving desired electrochemical performance. Table 2 summarizes the weight ratios of the materials used for the electrode slurry.



(a)



(b)

**Fig. 3.** (a) The process for making PVA polymer-based solid electrolyte, and (b) PVA

Following the preparation of all components, the electrode slurry was formulated. The active material, PVDF binder, and acetylene black conductive agent were weighed according to the designated ratios (Table 2). These components were then combined in an NMP solvent and subjected to vigorous agitation for a minimum of 5 hours. This extended mixing period ensured proper dispersion of all components throughout the slurry and minimized the formation of agglomerates. Subsequently, the slurry underwent an additional continuous stirring process for 2-3 hours to achieve optimal homogeneity. A conventional slurry coating technique was then employed to deposit the prepared slurry onto nickel foam current collectors. The nickel foam served as the substrate for the active material and facilitated efficient electron transport during subsequent electrochemical testing. Following coating, the electrodes were subjected to a drying process overnight to remove any residual solvent and ensure complete film formation. This drying step is crucial for maintaining the structural integrity of the electrode during electrochemical evaluation. The fully prepared electrodes were then ready for further characterization and testing. Figure 4 illustrates the movement of ions within the electrolyte and their interaction with the current collector.

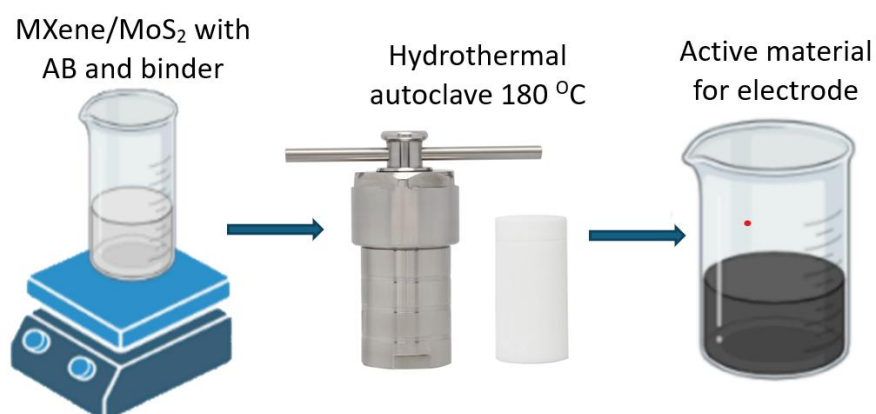


Fig. 4. Schematic representation of hydrothermal synthesis of MXene/MoS<sub>2</sub>

**Table 2**

The ionic conductivities of polymer electrolytes based on PVA

Sample	Weight (mg)	Weight Composition (%)
Mxene powder	8.30	40
MoS <sub>2</sub> powder	8.10	40
PVDF	1.28	10
Acetylene Black	1.26	10
Total weight	18.94	100

#### 2.4 Structural and Morphological Confirmation

The crystallinity of pristine MoS<sub>2</sub> and MXene/MoS<sub>2</sub> hybrid electrodes was analyzed using X-ray Diffraction (XRD). The analysis was performed with a Rigaku MiniFlex instrument, which utilized a monochromatic X-ray beam with a wavelength of 1.5406 Å. The diffraction patterns were collected over a 2θ range of 5° to 90°, and phase identification was conducted using the XPERT-PRO database. Raman spectroscopy was employed to investigate the vibrational modes of the materials, providing further insights into their structural characteristics and properties. The morphological analysis was conducted using field emission scanning electron microscopy (FESEM) with a Hitachi SU5000 microscope. This technique allowed for an examination of the surface morphology and internal structures of the materials.

#### 2.5 Electrochemical performance evaluation

For the electrochemical characterization, the fabricated electrodes were assembled into a symmetric supercapacitor configuration within a coin cell. A polyvinyl alcohol (PVA)-based solid electrolyte was chosen as the internal electrolyte, and polypropylene (PP) was used as the separator. Cyclic voltammetry (CV) and galvanostatic charge-discharge (GCD) measurements were performed using a WonAtech WMPG1000 electrochemical workstation. These measurements were crucial for evaluating the electrochemical performance of the fabricated supercapacitors. The comprehensive analysis aimed to provide a thorough understanding of the structural and electrochemical properties of the MXene/MoS<sub>2</sub> hybrid materials, highlighting their potential applications in energy storage devices.

### 3. Results and Discussion

#### 3.1 Morphological, Crystallographic Structure of Active Materials

Figure 5 shows the XRD patterns obtained from pristine MoS<sub>2</sub> and MXene/MoS<sub>2</sub> electrodes. Nevertheless, there are apparent variations in peak heights that correspond to the individual peaks, and fortunately both samples have good crystallinity [23]. The XRD spectrum pattern of an exfoliated pure MoS<sub>2</sub> electrode is shown. The data shows peaks at angles of 14.6°, 33°, 36.1°, 39.7°, 50°, and 60.6°, with corresponding d-spacing of 6.07, 2.72, 2.49, 2.27, 1.82, and 1.53Å. Minor peaks emerge at angles of 14.6, 33, 39.7, and 60.6°, which correspond to the MoS<sub>2</sub> crystal planes (002), (101), (103), and (110), correspondingly; this is consistent with the standard reference. A reduction to a lower intensity of peak at 2θ of 32.9, 36.1, and 50° from MoS<sub>2</sub> patterns can be detected by observing the achieved results of peaks of data varying from pure MoS<sub>2</sub> electrode up until MXene/MoS<sub>2</sub> hybrid electrode [24]. This shows the ability of MXene material to unload onto the exfoliated MoS<sub>2</sub> electrode. The lack of the Al peak around ~38° indicates the effective removal of the Al layer from the MAX phase material.

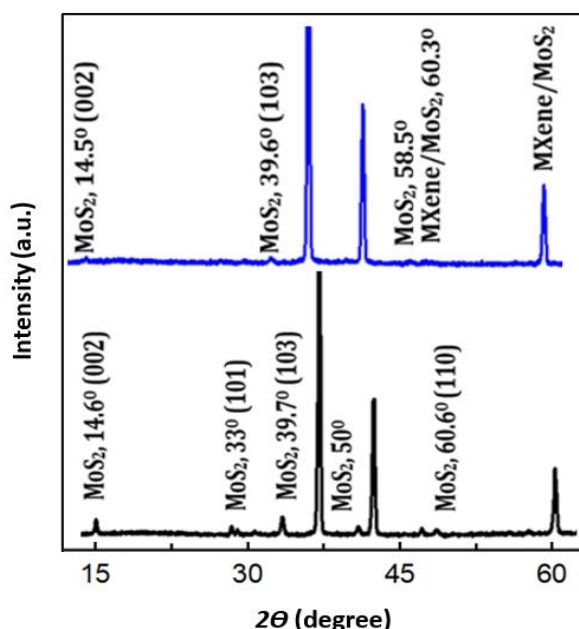


Fig. 5. XRD of MoS<sub>2</sub> and MXene/MoS<sub>2</sub> electrode

Both surfaces of the Ti<sub>3</sub>C<sub>2</sub> MXene are covered by a nanosheet composed of MoS<sub>2</sub>, as can be seen in the morphologies. The FESEM images shown in Figure 6 (a) and (b) revealed that the Ti<sub>3</sub>C<sub>2</sub> MXene exhibits a layered structure, consistent with its synthesis from the selective etching of aluminium layers from Ti<sub>3</sub>AlC<sub>2</sub>. The layered nature is a hallmark feature of MXenes and is evident as stacked sheets or flakes [25]. The surface topography appears relatively smooth, with some observable wrinkles and undulations. These features are attributed to the inherent flexibility and mechanical properties of MXene nanosheets [26]. Figure 6 (c) and (d) depict the morphological characteristics of pure MoS<sub>2</sub>. These samples showcase the presence of lamellar nanoflower-like MoS<sub>2</sub> structures. Lastly, Figure 7 (e) and (f) present images detailing the morphological features of hybrid MXene/MoS<sub>2</sub> structures. These images vividly illustrate the attachment of MoS<sub>2</sub> to the MXene, which plays an important role in effectively preventing the restacking of individual MoS<sub>2</sub> layers. It can be seen that MoS<sub>2</sub> materials are attached and fill the spaces between the Ti<sub>3</sub>C<sub>2</sub>. This phenomenon enhances the

utility of MXene in optimizing the structural integrity of MoS<sub>2</sub>, a point that is critical for further comprehensive understanding [27]. While Figure 7 shows XRD and Raman spectrum for materials in PVA based solid electrolyte which include KOH. The PVA pattern shows a big peak at  $2\theta=20^\circ$  and a secondary peak at  $40.5^\circ$ . These peaks indicate a certain extent of crystalline phase in pure PVA, which can be associated with polymer chains alignment due to H- bonds formed between OH<sup>-</sup> groups of packed PVA chains [28].

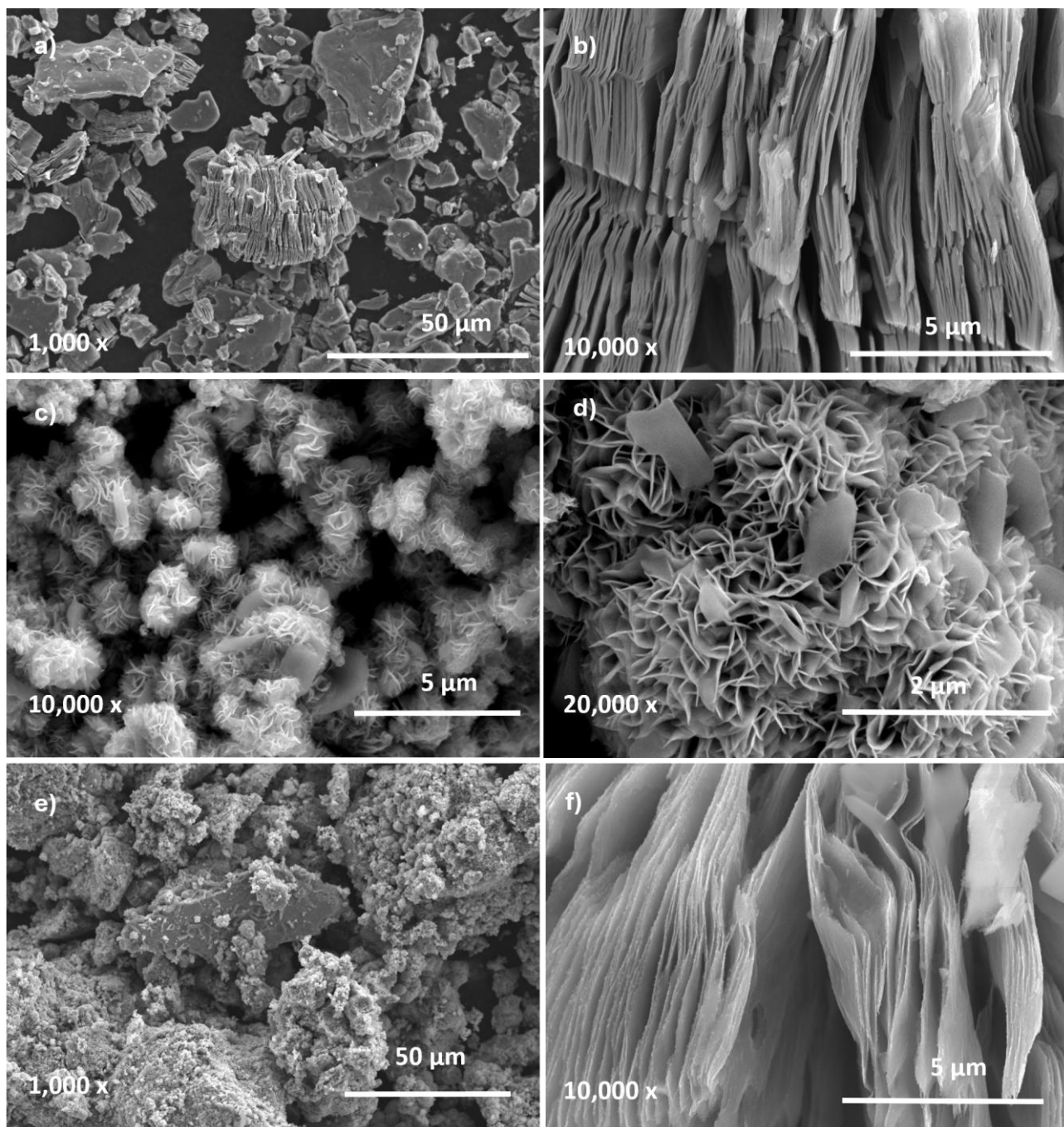
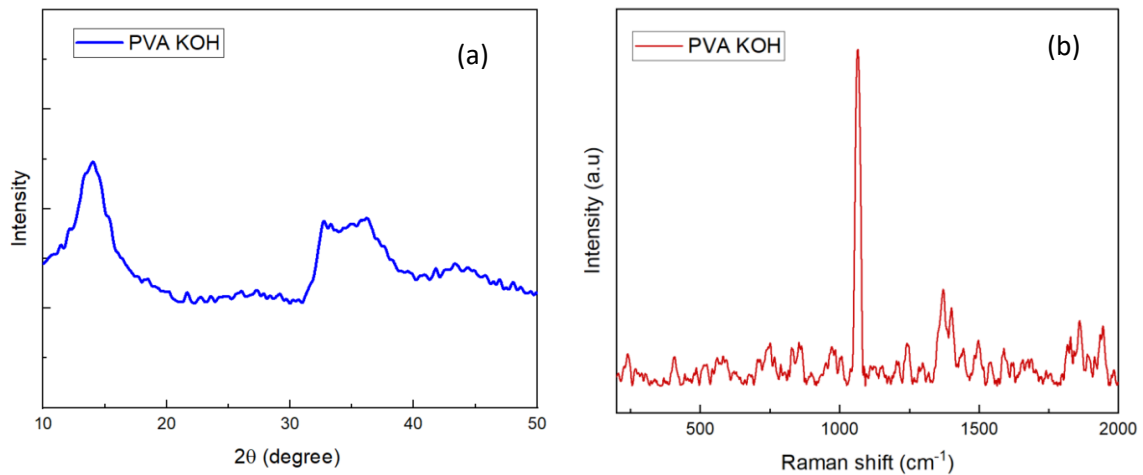


Fig. 6. FESEM images of a), b) Ti<sub>3</sub>C<sub>2</sub> MXene, c), d) MoS<sub>2</sub>, and e), f) MXene/MoS<sub>2</sub> electrode



**Fig. 7.** (a) XRD and (b) Raman spectrum of PVA solid electrolyte

#### 4. Electrochemical Performance of Supercapacitor

The cyclic stability of the MXene/MoS<sub>2</sub>-based supercapacitor was investigated through galvanostatic charge-discharge (GCD) measurements at a high current density of 0.793 A g<sup>-1</sup>. Capacity retention over extended cycling is a critical metric for evaluating the long-term viability of the MXene/MoS<sub>2</sub> electrode material in supercapacitor applications. Both cyclic voltammetry (CV) and GCD techniques are valuable tools for characterizing the capacitance of electrode materials. However, they offer distinct advantages and serve complementary purposes in this study. CV offers a relatively rapid method for initial assessments and preliminary screening of electrochemical properties. In contrast, GCD provides insights into the long-term stability and performance of the supercapacitor device under realistic operating conditions, mimicking the charge-discharge cycles encountered during practical use. For this study, the specific capacitance ( $C_{sp}$ ) obtained from CV measurements was employed to evaluate the performance of the fabricated supercapacitors. This choice allows for a quick and efficient initial assessment of the device's capacitance. The achieved CV curves are then discussed and used to calculate the specific gravimetric capacitance ( $C_{sp}$ ) value. Equation 1 to calculate the  $C_{sp}$  is as follows:

$$C_{sp1} = \frac{A}{mR(V_2 - V_1)} \quad (1)$$

where  $(V_2 - V_1)$  = potential window,  $m$  = average active mass per electrode,  $R$  = scan rates, and  $A$  = area under the curve, which was calculated by using Origin software from the CV voltammogram obtained in the experiment. In this study, the active mass is 0.0189 g.

From the GCD results, Equation 2 to calculate specific gravimetric capacitance ( $C_{sp}$ ):

$$\text{Specific Capacitance, } C_{sp2} = \frac{I \times \Delta t}{m \times \Delta V} = \frac{I_m(\Delta t)}{\Delta V} \quad (2)$$

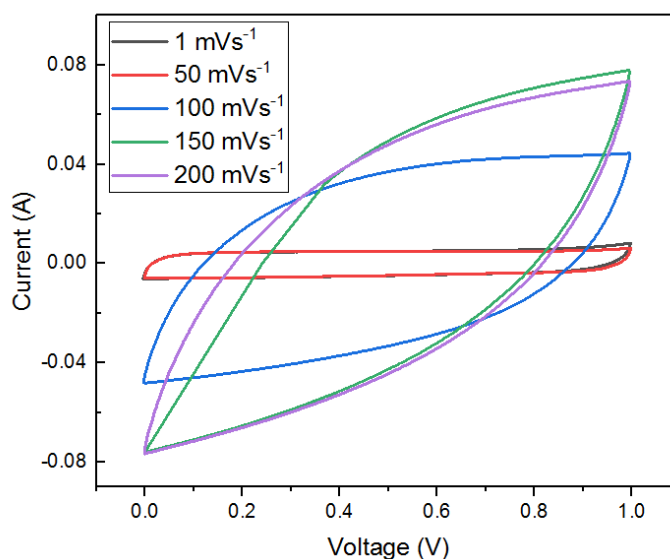
where  $I$  = current applied,  $m$  = average active mass of electrode,  $\Delta t$  = time difference,  $I_m$  = current densities, and  $\Delta V$  = voltage difference.

Figure 8 shows the CV curves of the MXene/MoS<sub>2</sub> symmetrical supercapacitor at different scan rates. The calculated  $C_{sp}$  values are presented and tabulated in Table 3. There is clearly no redox reaction peaks recorded, which indicates that the electrode exhibited good capacitive behaviour for a symmetric supercapacitor. The relatively not-so-high calculated  $C_{sp}$  value as compared to the literature data is most probably due to the high electrode loading or high active mass on the current collector [29]. Possibly, minimizing the electrode active mass might be a potential solution for achieving a high specific capacitance value. When the electrode loading is minimized, the whole or complete potential of each element inside the electrode may play a crucial role in enhancing the storage ability. Another matter to consider would be the coating technique applied during the preparation of the electrode [30]. Enhancing coating techniques in material synthesis holds significance for bolstering the future performance, durability, and functionality of coated materials.

**Table 3**

Specific gravimetric capacitance of MXene/MoS<sub>2</sub> hybrid electrode from CV analysis, calculated using (1)

Area under curves	Scan rates (mVs <sup>-1</sup> )	$C_{sp}$ (Fg <sup>-1</sup> )
0.009291	1	50.62
0.054250	50	29.56
0.069050	100	25.08
0.068820	150	18.75
0.068820	200	15.76



**Fig. 8.** CV curves of the MXene/MoS<sub>2</sub> symmetrical supercapacitor at different scan rates

The supercapacitor exhibited a quasi-rectangular-shaped curve for its CV, also confirming that this hybrid electrode shows good electrochemical double-layer capacitance (EDLC) behaviour [31]. When a lower scan rate was applied, the ion diffusion became slower; thus, the interaction between electrodes and electrolytes could be maximized. Also, the high-concentration electrolyte provides a higher number of ions, and when measured at a lower scan rate, the electrolyte ions have sufficient time to penetrate electrode pores and finally yield a better electrical charge storage for a good capacitance value [32]. Combining MXene and MoS<sub>2</sub> helped in increasing the active area, thus improving the charge–discharge process. Another reason for a lower  $C_{sp}$  is probably the synthesis method not involving the oxidation, which is known to hinder the performance of MXene.

On the other hand, higher scan rates allowed more current flow and led to quick ion diffusion, during which electrolyte ions were unable to fully penetrate electrode pores but only on the surface instead [33]. In contrast, when a lower value of scan rates is applied, the capability to capture the details is more accurate; thus, it takes longer to complete testing and yield a more accurate result. The galvanostatic charge–discharge data are depicted in Figure 9 and Table 4. The optimum current density ( $2.640 \text{ A g}^{-1}$ ) was selected based on the balance between high specific capacitance and rate performance. While lower current density ( $0.530 \text{ A g}^{-1}$ ) yielded higher capacitance, it lacked practical charge–discharge efficiency. Higher current density ( $5.280 \text{ A g}^{-1}$ ) showed significant capacitance loss due to limited ion diffusion. The selected value ensures efficient ion transport with stable cyclic behaviour, consistent with previous findings. The charging and discharging were found to be symmetric at around 30 secs for both charge and discharge. The unequal charge–discharge time indicated that the electrodes in such compositions are not really stabilized [34]. Furthermore, the  $C_{sp}$  values calculated using Equation (2) were very low, because of the high current applied, leading to too rapid a charge–discharge process, and this is common for symmetric supercapacitor.

**Table 4**  
 Specific capacitance of MXene/MoS<sub>2</sub> hybrid electrode from GCD analysis

Discharging time (sec)	Applied Current (mA)	Current Density ( $\text{A g}^{-1}$ )	Specific Capacitance ( $\text{F g}^{-1}$ )
56.01	1.0	0.530	29.69
7.08	5.0	2.640	18.48
3.12	10.0	5.280	1.650

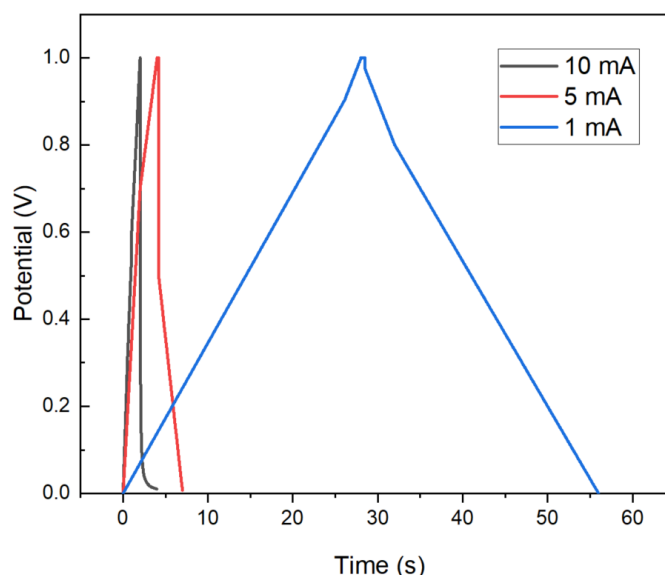


**Fig. 9.** GCD pattern of the MXene/MoS<sub>2</sub> hybrid electrode

Measurements were conducted to assess the specific capacitance of MXene/MoS<sub>2</sub>, spanning a total of 10,000 cycles as shown in Figure 10. Despite obtaining low specific capacitance ( $C_{sp}$ ) values from cyclic voltammetry (CV) and galvanostatic charge–discharge (GCD) tests, the material exhibited remarkable cyclic performance. The cyclic performance of MXene/MoS<sub>2</sub> was evaluated over 10,000 cycles at a current of 1.0 mA, within a voltage range of 0.0–1.0 V. The specific current density was selected as it represents an optimal value for the GCD parameters, neither excessively high nor too

low. In summary, the capacitance retention of MXene/MoS<sub>2</sub> after 2,000, 4,000, 6,000, and 8,000 cycles was observed to be 97.15%, 97.71%, 96.87%, and 95.75%, respectively.

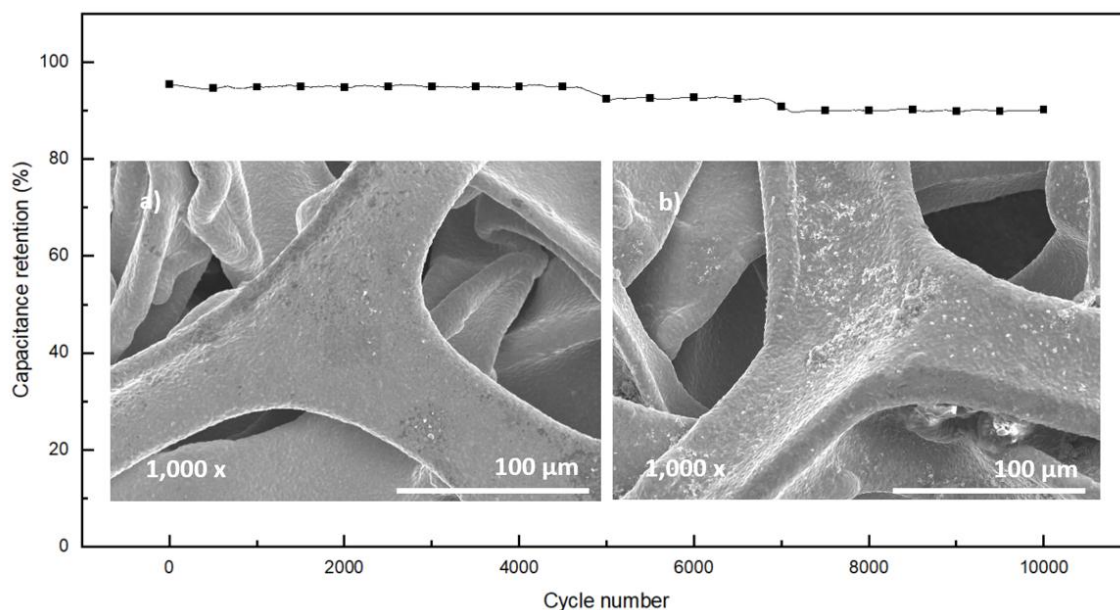


**Fig. 10.** Sample (a) before and (b) after 10,000 cycles capacitance retention evaluation

After subjecting the cell to 10,000 cycles of capacitance retention testing, a comprehensive assessment of its physical and electrochemical characteristics revealed no discernible changes [35]. This observed stability could be attributed to the stored energy resulting from the physical separation of charges, mitigating the chemical reactions typically associated with battery charge and discharge cycles. Chemical reactions often lead to material degradation and diminished performance over time. The image indicates that the sample has maintained its appearance, resembling a crumpled piece of paper, thus signifying its structural integrity during the retention tests. The reliable and stable capacitance retention observed after an extensive testing period underscores the cell's robust and enduring performance. It is an excellent choice for applications necessitating long-term and dependable cycle retention, such as advanced energy storage systems [36].

The MXene-MoS<sub>2</sub> combination shows beneficial interactions, as shown in the characterization results. MoS<sub>2</sub> nanosheets help separate MXene layers, increasing accessible surface area, while MXene's conductivity compensates for MoS<sub>2</sub>'s semiconductor nature. Spectroscopic data confirms electronic coupling between the materials. Together, they enable both surface charge storage and redox reactions. Even though the measured specific capacitance suggests room for improvement in the MXene/MoS<sub>2</sub>-PVA system. Three main factors likely contribute to this performance, which are, first, restricted ion movement in the PVA electrolyte due to its semi-crystalline structure [37]. Secondly, there is a reduced active surface area from MXene sheet stacking, and thirdly, there is interfacial resistance between components. Simple modifications could enhance performance, such as adding glycerol to PVA to improve ion mobility or incorporating carbon nanotubes between MXene layers to prevent restacking [38]. For better performance, future work could focus on optimizing the PVA electrolyte composition to balance flexibility and ion transport. Besides controlling MoS<sub>2</sub> morphology to expose more active edge sites and improving electrode-electrolyte contact through surface treatments. These practical adjustments could enhance capacitance while maintaining the system's stability and ease of fabrication. The current results provide a foundation for developing

more efficient solid-state supercapacitors using this material combination. Figure 11 illustrates the suggestion of ions' movement within the electrolyte and their interaction with the current collector.

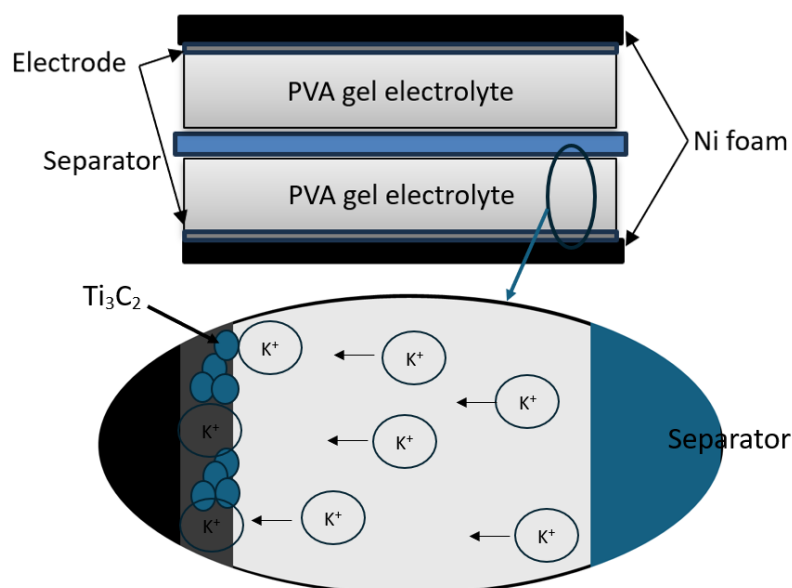


**Fig. 11.** Suggestion for schematic movement of  $K^+$  ion within the electrolyte and their interaction with the current collector

#### 4. Conclusions

The synthesis of the MXene/ $MoS_2$  hybrid electrode was achieved using a hydrothermal process followed by conventional slurry coating. XRD patterns verified the successful deposition of MXene  $Ti_3C_2$  onto the exfoliated  $MoS_2$  electrode, confirming the composite heterostructure's crystalline nature. FESEM analysis revealed that the  $Ti_3C_2$  MXene exhibited a layered flake-like structure, consistent with its formation through the selective removal of aluminum layers from  $Ti_3AlC_2$ . The electrochemical performance of the MXene/ $MoS_2$  supercapacitor was assessed through cyclic voltammetry (CV) and galvanostatic charge-discharge (GCD) tests, yielding a maximum specific capacitance of  $50.62 \text{ Fg}^{-1}$ . Subsequently, the device underwent 10,000 cycles of cyclic testing at an applied current of 1.0 mA, demonstrating a capacitance retention of 95.75% of its initial discharge capacitance. Notably, the cell remained unchanged even after enduring 10,000 retention cycles, underscoring its robust cyclic stability. It's important to note that the usage of PVA solid electrolytes significantly affected the performance of the supercapacitor, contributing to its enhanced stability and retention of capacitance over multiple cycles.

#### Acknowledgement

The authors are grateful to Universiti Teknikal Malaysia Melaka for the facilities support. Special thanks to the Ministry of Higher Education for financially supporting this research under the Fundamental Research Grant Scheme (FRGS) research grant numbered FRGS/1/2021/TK0/UTEM/01/3/F00476.

## References

- [1] Sun, Jie, Xuejian Li, Weiling Guo, Miao Zhao, Xing Fan, Yibo Dong, Chen Xu, Jun Deng and Yifeng Fu, "Synthesis Methods of Two-Dimensional MoS<sub>2</sub>: A Brief Review," *Crystals* 7, no. 7 (2017): 198. <https://doi.org/10.3390/cryst7070198>
- [2] Azam, Mohd Asyadi, Nik Suhaini Nik Ramli, Nurul Aini Nadirah Mohd Nor and Tuan Idzuddin Tuan Nawi, "Recent Advances in Biomass - derived Carbon, Mesoporous Materials, and Transition Metal Nitrides as New Electrode Materials for Supercapacitor: A Short Review," *International Journal of Energy Research* 45, no. 6 (January 3, 2021): 8335–46. <https://doi.org/10.1002/er.6377>
- [3] Pan, Zhongmou, Zeming Lu, Lang Xu and Dewei Wang, "A Robust 2D Porous Carbon Nanoflake Cathode for High Energy-power Density Zn-ion Hybrid Supercapacitor Applications," *Applied Surface Science* 510 (January 18, 2020): 145384. <https://doi.org/10.1016/j.apsusc.2020.145384>
- [4] Kirubasankar, Balakrishnan, Mugilan Narayanasamy, Jun Yang, Mingyu Han, Wenhuan Zhu, Yanjie Su, Subramania Angaiah and Chao Yan, "Construction of Heterogeneous 2D Layered MoS<sub>2</sub>/MXene Nanohybrid Anode Material via Interstratification Process and Its Synergetic Effect for Asymmetric Supercapacitors," *Applied Surface Science* 534 (August 27, 2020): 147644. <https://doi.org/10.1016/j.apsusc.2020.147644>
- [5] Gupta, Honey, S. Chakrabarti, Sagar Mothkuri, Balaji Padya, T.N. Rao and P.K. Jain, "High Performance Supercapacitor Based on 2D-MoS<sub>2</sub> Nanostructures," *Materials Today Proceedings* 26 (July 25, 2019): 20–24. <https://doi.org/10.1016/j.matpr.2019.04.198>
- [6] Tan, Kang Miao, Thanikanti Sudhakar Babu, Vigna K. Ramachandaramurthy, Padmanathan Kasinathan, Sunil G. Solanki and Shangari K. Raveendran, "Empowering Smart Grid: A Comprehensive Review of Energy Storage Technology and Application With Renewable Energy Integration," *Journal of Energy Storage* 39 (May 6, 2021): 102591. <https://doi.org/10.1016/j.est.2021.102591>
- [7] Vukajlović, Nikola, Dragan Milićević, Boris Dumnić and Bane Popadić, "Comparative Analysis of the Supercapacitor Influence on Lithium Battery Cycle Life in Electric Vehicle Energy Storage," *Journal of Energy Storage* 31 (June 11, 2020): 101603. <https://doi.org/10.1016/j.est.2020.101603>
- [8] Azam, Mohd Asyadi, None R.N.A.R. Seman, None M.A. Mohamed and M.H. Ani, "Effect of Polytetrafluoroethylene Binder Content on Gravimetric Capacitance and Life Cycle Stability of Graphene Supercapacitor," *International Journal of Automotive and Mechanical Engineering* 19, no. 3 (September 30, 2022): 9964–70. <https://doi.org/10.15282/ijame.19.3.2022.08.0768>
- [9] Balasubramaniam, Saravanakumar, Ankita Mohanty, Suresh Kannan Balasingam, Sang Jae Kim and Ananthakumar Ramadoss, "Comprehensive Insight Into the Mechanism, Material Selection and Performance Evaluation of Supercapatteries," *Nano-Micro Letters* 12, no. 1 (April 4, 2020). <https://doi.org/10.1007/s40820-020-0413-7>
- [10] Yang, Zefang, Lin Zhu, Chaonan Lv, Rui Zhang, Haiyan Wang, Jue Wang and Qi Zhang, "Defect Engineering of Molybdenum Disulfide for Energy Storage," *Materials Chemistry Frontiers* 5, no. 16 (January 1, 2021): 5880–96. <https://doi.org/10.1039/d1qm00442e>
- [11] Kosnan, Muhammad Akmal, Mohd Asyadi Azam, Nur Ezyanie Safie, Rose Farahiyan Munawar and Akito Takasaki, "Recent Progress of Electrode Architecture for MXene/MoS<sub>2</sub> Supercapacitor: Preparation Methods and Characterizations," *Micromachines* 13, no. 11 (October 27, 2022): 1837. <https://doi.org/10.3390/mi13111837>
- [12] Azam, M.A., Safie, N.E., Aziz, M.F.A., Seman, R.N.A.R. and Suhaili, M.R., "Structural Characterization and Electrochemical Performance of Nitrogen Doped Graphene Supercapacitor Electrode Fabricated by Hydrothermal Method," *International Journal of Nanoelectronics and Materials* 14, no. 2 (2021): 127-136.
- [13] Rehman, Javed, Xiaofeng Fan, Amel Laref, Van An Dinh and W.T. Zheng, "Potential Anodic Applications of 2D MoS<sub>2</sub> for K-ion Batteries," *Journal of Alloys and Compounds* 865 (January 23, 2021): 158782. <https://doi.org/10.1016/j.jallcom.2021.158782>
- [14] Krishnamoorthy, Karthikeyan, Ganesh Kumar Veerasubramani, Sivaprakasam Radhakrishnan and Sang Jae Kim, "Supercapacitive Properties of Hydrothermally Synthesized Sphere Like MoS<sub>2</sub> Nanostructures," *Materials Research Bulletin* 50 (November 12, 2013): 499–502. <https://doi.org/10.1016/j.materresbull.2013.11.019>

- [15] Kumar, Jagadeesan Aravind, Pandurangan Prakash, Thangavelu Krithiga, Duvuru Joshua Amarnath, Jayapal Premkumar, Natarajan Rajamohan, Yasser Vasseghian, Panchamoorthy Saravanan and Manivasagan Rajasimman, "Methods of Synthesis, Characteristics, and Environmental Applications of MXene: A Comprehensive Review," *Chemosphere* 286 (July 20, 2021): 131607. <https://doi.org/10.1016/j.chemosphere.2021.131607>
- [16] Panda, Subhasree, Kalim Deshmukh, S.K. Khadheer Pasha, Jayaraman Theerthagiri, Sivakumar Manickam and Myong Yong Choi, "MXene Based Emerging Materials for Supercapacitor Applications: Recent Advances, Challenges, and Future Perspectives," *Coordination Chemistry Reviews* 462 (March 28, 2022): 214518. <https://doi.org/10.1016/j.ccr.2022.214518>
- [17] Naguib, Michael, Michel W. Barsoum and Yury Gogotsi, "Ten Years of Progress in the Synthesis and Development of MXenes," *Advanced Materials* 33, no. 39 (August 16, 2021): 2103393. <https://doi.org/10.1002/adma.202103393>
- [18] Li, Zhong-Kun, Yanchang Liu, Libo Li, Yanying Wei, Jürgen Caro and Haihui Wang, "Ultra-thin Titanium Carbide (MXene) Sheet Membranes for High-efficient Oil/Water Emulsions Separation," *Journal of Membrane Science* 592 (August 9, 2019): 117361. <https://doi.org/10.1016/j.memsci.2019.117361>
- [19] Kim, Sung-Kon, Hyung-Jun Koo, Jinyun Liu and Paul V. Braun, "Flexible and Wearable Fiber Microsupercapacitors Based on Carbon Nanotube–Agarose Gel Composite Electrodes," *ACS Applied Materials & Interfaces* 9, no. 23 (May 24, 2017): 19925–33. <https://doi.org/10.1021/acsami.7b04753>
- [20] Jiang, Mengjin, Jiadeng Zhu, Chen Chen, Yao Lu, Yeqian Ge and Xiangwu Zhang, "Poly(Vinyl Alcohol) Borate Gel Polymer Electrolytes Prepared by Electrodeposition and Their Application in Electrochemical Supercapacitors," *ACS Applied Materials & Interfaces* 8, no. 5 (January 20, 2016): 3473–81. <https://doi.org/10.1021/acsami.5b11984>
- [21] Hashim, M.A. and A.S.A. Khair, "Supercapacitor Based on Activated Carbon and Hybrid Solid Polymer Electrolyte," *Materials Research Innovations* 15, no. sup2 (August 1, 2011): s63–66. <https://doi.org/10.1179/143307511x13031890747813>
- [22] Hatta, F. F., M. Z. A. Yahya, A. M. M. Ali, R. H. Y. Subban, M. K. Harun and A. A. Mohamad, "Electrical Conductivity Studies on PVA/PVP-KOH Alkaline Solid Polymer Blend Electrolyte," *Ionics* 11, no. 5–6 (September 1, 2005): 418–22. <https://doi.org/10.1007/bf02430259>
- [23] Xu, Xiaoxuan, Youqiang Xing and Lei Liu, "Construction of MoS<sub>2</sub>-ReS<sub>2</sub> Hybrid on Ti3C<sub>2</sub>T<sub>x</sub> MXene for Enhanced Microwave Absorption," *Micromachines* 14, no. 11 (October 27, 2023): 1996. <https://doi.org/10.3390/mi14111996>
- [24] Bashir, Tariq, Shaowen Zhou, Shiqi Yang, Sara Adeeba Ismail, Tariq Ali, Hao Wang, Jianqing Zhao and Lijun Gao, "Progress in 3D-MXene Electrodes for Lithium/Sodium/Potassium/Magnesium/Zinc/Aluminum-Ion Batteries," *Electrochemical Energy Reviews* 6, no. 1 (March 1, 2023). <https://doi.org/10.1007/s41918-022-00174-2>
- [25] Kang, Minji, Yeong-A. Kim, Jin-Mun Yun, Dongyoon Khim, Jihong Kim, Yong-Young Noh, Kang-Jun Baeg and Dong-Yu Kim, "Stable Charge Storing in Two-dimensional MoS<sub>2</sub>nanoflake Floating Gates for Multilevel Organic Flash Memory," *Nanoscale* 6, no. 21 (August 11, 2014): 12315–23. <https://doi.org/10.1039/c4nr03448a>
- [26] Jahan, Nushrat, Salim Hussain, Huzef Ur Rahman, Insha Manzoor, Shashank Pandey, Kamran Habib, Syed Kaabir Ali, Reetika Pandita and Chandramani Upadhyay, "Structural, Morphological and Elemental Analysis of Selectively Etched and Exfoliated Ti<sub>3</sub>AlC<sub>2</sub> MAX Phase," *Journal of Multidisciplinary Applied Natural Science* 1, no. 1 (January 8, 2021): 13–17. <https://doi.org/10.47352/jmans.v1i1.6>
- [27] Luo, Shilu, Tiantian Xiang, Jingwen Dong, Fengmei Su, Youxin Ji, Chuntai Liu and Yuezhan Feng, "A Double Crosslinking MXene/Cellulose Nanofiber Layered Film for Improving Mechanical Properties and Stable Electromagnetic Interference Shielding Performance," *Journal of Material Science and Technology* 129 (May 28, 2022): 127–34. <https://doi.org/10.1016/j.jmst.2022.04.044>
- [28] Zhang, Ning, Bin Zhang, Yong Pang, Hong-Sheng Yang, Lu Zong, Yong-Xin Duan and Jian-Ming Zhang, "High Performance of PVA Nanocomposite Reinforced by Janus-like Asymmetrically Oxidized Graphene: Synergetic Effect of H-bonding Interaction and Interfacial Crystallization," *Chinese Journal of Polymer Science* 40, no. 4 (January 19, 2022): 373–83. <https://doi.org/10.1007/s10118-022-2664-x>
- [29] Najib, Sumaiyah and Emre Erdem, "Current Progress Achieved in Novel Materials for Supercapacitor Electrodes: Mini Review," *Nanoscale Advances* 1, no. 8 (January 1, 2019): 2817–27. <https://doi.org/10.1039/c9na00345b>

- [30] Naguib, Michael, Olha Mashtalir, Maria R. Lukatskaya, Boris Dyatkin, Chuanfang Zhang, Volker Presser, Yury Gogotsi and Michel W. Barsoum, "One-step Synthesis of Nanocrystalline Transition Metal Oxides on Thin Sheets of Disordered Graphitic Carbon by Oxidation of MXenes," *Chemical Communications* 50, no. 56 (January 1, 2014): 7420–23. <https://doi.org/10.1039/c4cc01646g>
- [31] M, Arunkumar and Amit Paul, "Importance of Electrode Preparation Methodologies in Supercapacitor Applications," *ACS Omega* 2, no. 11 (November 16, 2017): 8039–50. <https://doi.org/10.1021/acsomega.7b01275>
- [32] Maher, Mahmoud, Sameh Hassan, Kamel Shoueir, Bedir Yousif and Mohy Eldin A. Abo-Elhoud, "Activated Carbon Electrode With Promising Specific Capacitance Based on Potassium Bromide Redox Additive Electrolyte for Supercapacitor Application," *Journal of Materials Research and Technology* 11 (February 2, 2021): 1232–44. <https://doi.org/10.1016/j.jmrt.2021.01.080>
- [33] Norouzi, Omid, S. E. M. Pourhosseini, Hamid Reza Naderi, Francesco Di Maria and Animesh Dutta, "Integrated Hybrid Architecture of Metal and Biochar for High Performance Asymmetric Supercapacitors," *Scientific Reports* 11, no. 1 (March 8, 2021). <https://doi.org/10.1038/s41598-021-84979-z>
- [34] Cho, Sangwon, Junyoung Lim and Yongsok Seo, "Flexible Solid Supercapacitors of Novel Nanostructured Electrodes Outperform Most Supercapacitors," *ACS Omega* 7, no. 42 (October 12, 2022): 37825–33. <https://doi.org/10.1021/acsomega.2c04822>
- [35] Tawiah, Benjamin, Raphael Kanyire Seidu, Benjamin Kwablah Asinyo and Bin Fei, "A Review of Fiber-based Supercapacitors and Sensors for Energy-autonomous Systems," *Journal of Power Sources* 595 (January 13, 2024): 234069. <https://doi.org/10.1016/j.jpowsour.2024.234069>
- [36] Lei, Yu, Da Han, Jiahui Dong, Lei Qin, Xiaojing Li, Dengyun Zhai, Baohua Li, Yiyang Wu and Feiyu Kang, "Unveiling the Influence of Electrode/Electrolyte Interface on the Capacity Fading for Typical Graphite-based Potassium-ion Batteries," *Energy Storage Materials* 24 (August 1, 2019): 319–28. <https://doi.org/10.1016/j.ensm.2019.07.043>
- [37] Aslam, Muhammad, Mazhar Ali Kalyar and Zulfiqar Ali Raza, "Polyvinyl Alcohol: A Review of Research Status and Use of Polyvinyl Alcohol Based Nanocomposites," *Polymer Engineering and Science* 58, no. 12 (April 10, 2018): 2119–32. <https://doi.org/10.1002/pen.24855>
- [38] Brza, Mohamad A., Shujahadeen B. Aziz, Hazleen Anuar, Elham M. A. Dannoun, Fathilah Ali, Rebar T. Abdulwahid, Shakhawan Al-Zangana and Mohd F.Z. Kadir, "The Study of EDLC Device With High Electrochemical Performance Fabricated From Proton Ion Conducting PVA-Based Polymer Composite Electrolytes Plasticized With Glycerol," *Polymers* 12, no. 9 (August 23, 2020): 1896. <https://doi.org/10.3390/polym12091896>
- [39] Radhakrishnan, Sithara, Seetha Lakshmy, K.A. Sree Raj, Brahmananda Chakraborty, Jung Sang Cho, Sang Mun Jeong and Chandra Sekhar Rout, "Facile and Scalable Fabrication of Flexible Microsupercapacitor Based on Boron Modified 2D/2D 1 T MoS<sub>2</sub>/MXene Hybrids," *Journal of Energy Storage* 99 (August 25, 2024): 113478. <https://doi.org/10.1016/j.est.2024.113478>
- [40] Alam, Md. Rubel, Mitu Gharami, Barshan Dev, Md Ashikur Rahman and Tarikul Islam, "Next - Generation Materials for Multifunctional Applications: Design Progress and Prospects of 2D MXene - Enabled Hybrid Architectures," *Advanced Materials Interfaces*, January 2, 2025. <https://doi.org/10.1002/admi.202400681>
- [41] Safie, Nur Ezyanie, Mohd Asyadi Azam, Chun Khean Chiew, Mohd Fareezuan Abdul Aziz, Mohamad Nazmi Faiz Md Sairi and Akito Takasaki, "Structural Characterizations and Electrochemical Performances of rGO-based Anode Materials for Lithium-ion Battery," *Journal of Materials Science Materials in Electronics* 34, no. 30 (October 1, 2023). <https://doi.org/10.1007/s10854-023-11398-3>
- [42] Shin, Jae Hyuk, Su Hun Jo, Hyejin Rhyu, Chanwon Park, Myung Hyun Kang, Wooseok Song, Sun Sook Lee, Jongsun Lim and Sung Myung, "High-performance H<sub>2</sub>S Gas Sensor Utilizing MXene/MoS<sub>2</sub> Heterostructure Synthesized via the Langmuir–Blodgett Technique and Chemical Vapor Deposition," *RSC Advances* 14, no. 51 (January 1, 2024): 37781–87. <https://doi.org/10.1039/d4ra07555b>
- [43] Tyagi, Nahid, Manoj Kumar Singh, Sudheshna Moka and Manika Khanuja, "Facile Synthesis of MXene From MAX Phase via Hydrothermal Method Using a Mild Etchant," *Hybrid Advances* 7 (August 27, 2024): 100285. <https://doi.org/10.1016/j.hybadv.2024.100285>

- [44] Guo, Teng, Yuan Lei, Xin Hu, Guang Yang, Jie Liang, Qiang Huang, Xiancai Li, Meiyong Liu, Xiaoyong Zhang and Yen Wei, "Hydrothermal Synthesis of MXene-MoS<sub>2</sub> Composites for Highly Efficient Removal of Pesticides," *Applied Surface Science* 588 (February 17, 2022): 152597. <https://doi.org/10.1016/j.apsusc.2022.152597>
- [45] Zargar, Seyed Ali, Masoud Dehghani Mohammad Abadi, Elham Soroush, Adrine Malek Khachatourian, Mohammad Golmohammad and Ali Nemati, "Synthesis of Novel 2D/2D Ti<sub>3</sub>C<sub>2</sub>T<sub>x</sub> MXene / 1T-MoS<sub>2</sub> Heterostructure Enhanced With Carbon Nanotubes as a Highly-efficient Electrode for Hybrid Capacitive Deionization," *Journal of Alloys and Compounds* 981 (February 3, 2024): 173765. <https://doi.org/10.1016/j.jallcom.2024.173765>